Self-Consistent Field Theory of Block Copolymers with Conformational Asymmetry

J. D. Vavasour

Department of Physics, University of British Columbia, Vancouver, BC, Canada V6T 1Z1

M. D. Whitmore*

Department of Physics, Memorial University of Newfoundland,
St. John's, NF, Canada A1B 3X7

Received May 3, 1993; Revised Manuscript Received September 28, 1993®

ABSTRACT: Using self-consistent mean field theory, we have investigated the effects of conformational asymmetry on the phase diagram of diblock copolymers, considering spherical, cylindrical and lamellar microphases. This asymmetry, which reflects the mismatch of the pure component densities and Kuhn statistical lengths for the two blocks, is characterized by a single additional parameter. We calculated one phase diagram for systems with asymmetry corresponding approximately to copolymers such as PS-*b*-PI or PS-*b*-PBD, and a second one for a system with high asymmetry. In addition to shifting the microphase boundaries, it opens up direct windows from the disordered phase to the lamellar and cylindrical phases on one side of the phase diagram.

1. Introduction

In broad terms, the microphase behavior of A-*b*-B diblock copolymers is now generally understood. They can undergo an order–disorder transition, frequently referred to as the microphase separation transition (MST), as well as a number of order–order transitions. Four ordered microphases are well-known, which consist of alternating layers which we denote L, cylinders on a hexagonal lattice, C, spheres on a body centered cubic lattice, S, and a bicontinuous "double diamond" structure, OBDD.[1,2] In addition, there is now considerable evidence of other structures near the order–disorder transition.[3,4]

The full specification of such a system of monodisperse copolymers requires at least seven independent quantities, which we can identify as the copolymer degree of polymerization Z, the volume fraction of either diblock, f_A or $f_B = 1\text{-}f_A$, the two Kuhn statistical lengths b_A and b_B, the pure component densities ρ_{0A} and ρ_{0B}, and the Flory χ parameter (defined with respect to a reference density ρ_0). In addition, one could introduce the range of the interactions, but this appears to have little effect on the microphase diagram[5,6] and is frequently taken to be zero.

In the strong segregation regime, i.e., far from the MST, the equilibrium phases are believed to depend on only one of these seven quantities, the volume fraction of one of the blocks. A very widely studied system is PS-*b*-PI, for which the microphase boundaries have been summarized in detail by Bates and co-workers. Until very recently, it was believed that the S, C, OBDD, and L structures were all stable in the strong segregation regime,[7] but he and co-workers have recently suggested that, in strong segregation, the OBDD is only metastable.[8] Expressed in terms of the PS block, the stable phases are considered to be S for $f_{PS} \lesssim 0.17$, C for $0.17 \lesssim f_{PS} \lesssim 0.30$, L for $0.30 \lesssim f_{PS} \leq 0.64$, C for $0.64 \lesssim f_{PS} \lesssim 0.77$, and S for $f_{PS} \gtrsim 0.77$. The OBDD appears as a relatively narrow band near $f_{PS} \simeq 0.64$ and perhaps near $f_{PS} \simeq 0.30$. It should be noted that none of these boundaries are symmetric about $f_{PS} = 0.5$.

The behavior in weak segregation appears to be more complicated, with other phases, including the OBDD, becoming stable near the order–disorder transition. Furthermore, the equilibrium phase depends on both volume fraction and temperature: for certain volume fractions, the equilibrium phase changes with temperature.[3,4] As in strong segregation, the phase behavior is asymmetric in f_{PS}.

Our understanding of these systems is based on a variety of theoretical treatments. A common prediction of them all, however, is that the equilibrium microphase is determined primarily by only two quantities. In particular, for the special case $\rho_{0A} = \rho_{0B}$ and $b_A = b_B$, mean field theory predicts that the equilibrium phase depends *exclusively* on χZ and f_A,[6] and the behavior can be expressed in terms of a simple phase diagram such as Figure 1 of this paper.

One of the earliest calculations of the microphase diagram of block copolymers was the self-consistent field treatment of Helfand and Wasserman.[9] Their approach was similar to that used in the current paper, but also used the narrow interphase approximation (NIA), and so is restricted in applicability to the strong segregation regime. They used Kuhn lengths and pure component densities for PS-*b*-PBD and found order–order phase boundaries which were nearly independent of χ. Specifically, they obtained four phase boundaries corresponding to the sequence S ↔ C ↔ L ↔ C ↔ S occurring at PS weight fractions of about 0.1, 0.3, 0.65, and 0.85, respectively, which can be compared with the experimental values of 0.17, 0.30, 0.64, and 0.77 for PS-*b*-PI quoted above. In particular, the asymmetry in the experimental and theoretical results is similar: the phase boundaries are shifted toward lower PS content.

The earliest treatment of the weak segregation regime was by Leibler, who considered idealized systems with $\rho_{0A} = \rho_{0B}$ and $b_A = b_B$.[10] He developed an RPA theory based on a fourth order expression for the free energy and an assumed cosine-like order parameter. He predicted that the MST occurs at a value of χZ which depends on f_A and that all the order–order phase boundaries curve in the vicinity of the MST, merging with each other and with the MST at the point $\chi Z = 10.5$, $f_A = 0.5$. For all copolymers with $f_A \neq 0.5$, then as a function of increasing χZ the first equilibrium microphase consisted of spheres. Representing the disordered, or homogeneous, phase by H, we denote this transition by H ↔ S. This would be followed by

---

® Abstract published in *Advance ACS Abstracts,* November 1, 1993.

0024-9297/93/2226-7070$04.00/0

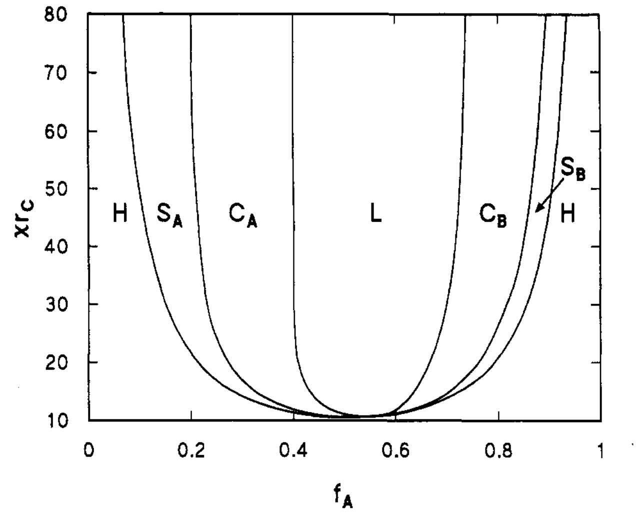

Figure 1. Calculated phase diagrams for copolymers with pure component densities and Kuhn statistical lengths chosen so $\epsilon \equiv (\rho_{0B}b_B^2)/(\rho_{0A}b_A^2) = 0.6$. To the extent that the dilution approximation applies, it would also correspond to a copolymer/neutral solvent blend with χr_C replaced with $\chi_{eff}r_C$.

transitions to cylinders and then to lamellae. Such a sequence of phases is qualitatively consistent with the observations of Almdal et al.[3] on PEP-*b*-PEE with volume fraction $f_{PEP} = 0.65$, as well as the more recently reported results.[4] However, the observed structures were more complicated than those treated theoretically and, perhaps more importantly, this sequence H ↔ S ↔ C ↔ L was predicted to occur for any $f_A \neq 0.5$. This means that there would be no direct "windows" from the disordered phase directly to the lamellar or cylindrical phases, except for the special case $f_A = 0.5$.

Fredrickson and Helfand[11] and Mayes and Olvera de la Cruz[12-14] extended the theory of Leibler, incorporating fluctuation effects. They found that Z enters as an additional independent variable controlling the microphase behavior. For finite Z, small H ↔ C and H ↔ L windows developed. However, as these windows appeared, the S region on the phase diagram, already very small in the Leibler theory, diminished and in fact disappeared for $Z \lesssim 10^4$.

All of the theories discussed above assumed the systems to be incompressible and all those for the weak segregation regime are for the idealized case $\rho_{0A} = \rho_{0B}$ and/or $b_A = b_B$. Tang, Freed, and Dudowicz have presented a theory of copolymers in the weak segregation regime, treating *compressible* systems, and ones in which $\rho_{0A} \neq \rho_{0B}$ and/or $b_A \neq b_B$. Their focus was on scattering from the disordered phase and on the order–disorder transition, but not on competing, ordered phases.

We recently calculated the microphase diagram using self-consistent field theory, also for the idealized systems with $\rho_{0A} = \rho_{0B}$ and $b_A = b_B$, but without the narrow interphase approximation or the truncation of the free energy to fourth order.[6] This method reduces to that of Helfand and Wasserman in the limit of strong segregation and to that of Leibler in weak segregation and near $f_A \simeq 0.5$, thus providing a unified mean field treatment of the entire phase diagram. For $\chi Z \gtrsim 70$, we found order–order phase boundaries which were almost independent of χZ, approaching limiting values of about $f_A \simeq 0.15$ and 0.33 for the S ↔ C and C ↔ L transitions, respectively. (In this system the phase boundaries are symmetric about $f_A = 0.5$.) These limits agree very well with those predicted for these idealized systems by the NIA, which we calculated using the program published by Helfand and Wasserman.[9] For progressively smaller values of χZ, all the phase boundaries curved and eventually merged at $\chi Z = 10.5$, $f_A = 0.5$, as in the Leibler theory. Again, there were no direct H ↔ C or H ↔ L windows except at the single point $f_A = 0.5$. However, the phase boundaries reduced quantitatively to Leibler's only in the range $0.45 \lesssim f_A \lesssim 0.55$. Beyond there, the S ↔ C and C ↔ L boundaries turned upward more quickly. In fact, the S and C regions of the phase diagram were considerably larger and the L region correspondingly smaller than those predicted by any previous theories for the weak segregation regime.

The dependence of the equilibrium phase on f_A has its obvious roots in the dissimilarity of the two blocks. However, there is another measure of this dissimilarity, which can be expressed in terms of the conformational asymmetry and refers to the possible mismatch between the volume fractions of the two blocks constituting each copolymer and their unperturbed radii of gyration. For example, even for a copolymer with $f_A = f_B = 0.5$, the unperturbed radii of gyration would, in general, differ due to unequal Kuhn lengths and/or monomer volumes. In a layered structure, the two subdomains would have equal thicknesses, but the deformations of the blocks from their corresponding unperturbed dimensions would differ. Mathematically, the two volume fractions satisfy

$$\frac{f_A}{f_B} = \frac{Z_A\rho_{0B}}{Z_B\rho_{0A}} \tag{1.1}$$

whereas the unperturbed radii of gyration satisfy

$$\frac{R_{A,g}^{\ 2}}{R_{B,g}^{\ 2}} = \frac{Z_A b_A^{\ 2}}{Z_B b_B^{\ 2}} \tag{1.2}$$

These two ratios need not be equal, which is what we mean by conformational asymmetry. The effects of this asymmetry are the subject of investigation in this paper.

Included in our recent work on the self-consistent field treatment of copolymers was the demonstration that, as long as the unit cell of each competing sructure can be described in terms of one lattice parameter, then within mean field theory the effects of conformational asymmetry can be included with just one extra quantity.[6] It can be taken to be the ratio of the two characteristics defined by eqs 1.1 and 1.2:

$$\begin{aligned}\epsilon &= \left(\frac{f_A}{f_B}\right)\Bigg/\left(\frac{R_{A,g}^{\ 2}}{R_{B,g}^{\ 2}}\right)\\ &= (\rho_{0B}b_B^{\ 2})/(\rho_{0A}b_A^{\ 2})\end{aligned} \tag{1.3}$$

This ratio characterizes the conformational asymmetry of a system, in terms of the densities and Kuhn lengths of the two components. For any real system, its value can be chosen to be either less than or greater than one through the identification of the A and B blocks. Note that conformational asymmetry can arise from differences in either the densities or the Kuhn lengths, or both. Conversely, even if the two blocks have unequal densities and Kuhn lengths, the copolymer could, in principle, be conformationally symmetric if the product $\rho_0 b^2$ is the same for both blocks.

This or similar ratios have been previously recognized as important. It was identified as a characteristic determining the scattering from disordered copolymers.[17] Furthermore, ϵ is similar to the asymmetry parameter introduced by Almdal et al.,[3] which is the ratio of effective statistical lengths calculated by assuming equal monomer densities. With a suitable definition of the monomer

Table I. Typical Values of Polymer Characteristics

	densities, ρ_0 (nm^{-3})		Kuhn lengths, b (nm)			$\rho_0 b^2$ (nm^{-1})		
PS	6.08^{a-e}	5.6^{f}	$0.68^{a-d,g,h}$	0.70^{f}		2.8^{a-d}	2.7^{f}	
PI	$8.2^{a,c,d}$		0.63^{a}	0.59^{c}	$0.67^{d,g}$	3.3^{a}	2.9^{c}	3.7^{d}
PBD	$9.9^{a,d,i}$	10.4^{f}	0.63^{a}	0.53^{d}	$0.65^{f,g}$	3.9^{a}	2.8^{d}	4.4^{f}
PMMA	8.9^{g}		0.74^{h}			4.9^{j}		
POE	17^{g}		0.7^{g}			8.3^{g}		

[a] Used in ref 9. [b] Reference 18. [c] Reference 19. [d] Reference 20. [e] Reference 21. [f] Reference 22. [g] Reference 23. [h] Reference 24. [i] Reference 25. [j] Calculated from entries *g* and *h*.

Table II. Asymmetry Ratios, $\epsilon = \rho_{0B} b_B^2 / \rho_{0A} b_A^2$, Calculated Using the Polymer Characteristics Listed in Table I[a]

copolymer	asymmetry ratio, ϵ		
PS-*b*-PI	$1.2^{a,a}$	$1.0^{c,c}$	$1.3^{d,d}$
PS-*b*-PBD	$1.4^{a,a}$	$1.0^{d,d}$	$1.6^{f,f}$
PI-*b*-PBD	$1.2^{a,a}$	$0.8^{d,d}$	$1.5^{c,f}$
PS-*b*-PMMA	$1.8^{a,j}$		
PS-*b*-POE	$3^{a,g}$		

[a] In each case, block A is the first of the pair, e.g., PS in PS-*b*-PI, and the superscripts identify the values (ρ_0 and b) from Table I used to calculate each ratio.

density, their ratio is equivalent to $\sqrt{\epsilon}$, and so has the same physical significance.

The existence of this as a controlling parameter implies that, even within mean field theory, there is no "universal", two dimensional phase diagram. Instead, the phase behavior is controlled by three characteristics, which can be taken to be χr_c, f_A, and ϵ. Here r_c is given by

$$r_c = \rho_0[Z_A/\rho_{0A} + Z_B/\rho_{0B}] \tag{1.4}$$

where ρ_0 is the reference density used in defining the Flory χ parameter. It can be interpreted as an effective degree of polymerization, and r_c/ρ_0 is the volume occupied by one molecule. The ρ_0 is normally related to ρ_{0A} and ρ_{0B}, but in any case the product χr_c is independent of its value.

The value of ϵ and hence the location of the phase boundaries depend on, but are not necessarily uniquely determined by, the copolymer chemical species. In particular, differing microstructures in two different samples of the same species can produce different conformational asymmetries. Thus the important quantity is ϵ; for a fixed ϵ, the phase behavior can be expressed as a function of χr_c and f_A, corresponding to a generalization of the χZ vs f_A phase diagram often exhibited. The idealized system with $b_A = b_B$ and $\rho_{0A} = \rho_{0B}$ corresponds to $\epsilon = 1$ with r_c reducing to $Z_A + Z_B = Z$.

The role of ϵ also extends to copolymer/neutral solvent blends. In an earlier paper we calculated the microphase diagram of such blends for conformationally symmetric copolymers, using a similar mean field, self-consistent theory.[5] The resulting phase diagram was virtually the same as for neat copolymers, when expressed in terms of an effective χ parameter given by $\chi_{\text{eff}} = \chi\bar{\phi}_c$, where $\bar{\phi}_c$ is the overall copolymer volume fraction. This result, which is simply the dilution approximation, can be related to the fact that the solvent density remained almost uniform throughout the system. If we assume *a priori* that the solvent density remains constant, then for blends with conformationally symmetric or asymmetric copolymers, we can incorporate the necessary changes to the self-consistent formalism by rescaling the incompressibility condition to $\phi_A(\mathbf{r}) + \phi_B(\mathbf{r}) = \bar{\phi}_c$. The consequence is that the new parameter, ϵ, plays the same role as in neat copolymers, and the microphase diagram is controlled by $\chi_{\text{eff}} r_c$, f_A, and ϵ. This result is, of course, limited to the concentrated regime, since it neglects the swelling effects of the solvent.

In order to identify realistic values of ϵ, we turned to the literature for typical values of reference densities and Kuhn lengths for some common polymers. These are shown in Table I. From the data displayed, it is apparent that in at least some cases, including PI and PBD, there is a range of quoted values for the Kuhn length in particular, and this variation implies differences in the resulting product $\rho_0 b^2$. In Table II we show values of ϵ calculated from the entries of Table I. Where possible, in constructing Table II we used characteristics for the two corresponding blocks taken from the same source. Even so, a significant range of values for ϵ persisted for each of the three cases for which we found multiple values for the quoted Kuhn length. For example, even for PS-*b*-PI, one value indicates no conformational asymmetry at all ($\epsilon \simeq 1.0$), while another value indicates $\epsilon \simeq 1.3$. For PS-*b*-PBD the variation is even larger, with ϵ ranging from 1.0 to 1.6. PI-*b*-PBD is particularly problematic, with ϵ ranging from less than unity to 1.5. Overall, the range is from about 0.8 to 3; this latter value also corresponds to the conformational asymmetry recently assigned to PE–PEP.[4] Since each value of ϵ and its multiplicative inverse are physically equivalent through the simple interchange of the A and B blocks, we have an equivalent range of about $0.3 \lesssim \epsilon \leq 1$. In the rest of this paper we restrict consideration to $\epsilon \leq 1$.

To the extent that variations in measured Kuhn lengths reflect the uncertainty in their measurements, this makes theoretical/experimental comparison more difficult. However, to the extent that these variations reflect real differences in the experimental systems, they introduce a more fundamental problem, namely that the actual phase boundaries would vary from sample to sample, even for the same chemical species. There would, for example, be no single phase diagram even for PS-*b*-PI.

The primary goal of this paper is to calculate the effects of conformational asymmetry on the microphase diagram of diblock copolymers, from the weak to the strong segregation regime, using self-consistent field theory. Our primary result is a phase diagram for the case $\epsilon = 0.6$, which lies well within the range indicated by the data of Table II. For this case we compare the results with our earlier ones for $\epsilon = 1$, with the Helfand and Wasserman strong segregation results which correspond to about $\epsilon = 0.7$, and with the published phase boundaries for PS-*b*-PI. We also construct a phase diagram for a case of particularly high conformational asymmetry, $\epsilon = 0.1$, which enhances the effects of asymmetry on the phase diagram in weak segregation. We have considered spheres, cylinders, and layers, since self-consistent calculations for the more complicated structures, including the OBDD, are beyond our current computational capability. It is also worth emphasizing that fluctuation effects are neglected in this approach. The desirability of incorporating them within the self-consistent field formalism, especially near the MST, is discussed in ref 6.

2. Formalism

A system of copolymers was specified by the degrees of polymerization, Kuhn statistical lengths and pure component densities for each block, and the Flory χ parameter. For each system we carried out self-consistent calculations of the equilibrium free energy and domain size for each of the three candidate microphases. The one with the lowest free energy was identified as the equilibrium morphology.

The calculations are a direct application of the mean field, self-consistent field formalism presented in Appendix

I of ref 6. For each microphase considered, the system was assumed to form a periodic structure, described by a set of lattice vectors $\mathbf{R}_n$, with an associated lattice constant R. The unit cells are layers for the lamellar phase; for the other structures we approximated them by cylinders or spheres. We needed to solve modified diffusion equations for propagators for each block. The propagators satisfy

$$[-\epsilon_p\beta\nabla^2 + \omega_p(\mathbf{r})]Q_p(\mathbf{r},\tau|\mathbf{r}') = -\frac{1}{f_p}\frac{\partial}{\partial\tau}Q_p(\mathbf{r},\tau|\mathbf{r}') \tag{2.5}$$

where

$$\beta = \frac{r_C\rho_{0A}{b_A}^2}{6\rho_0R^2} \tag{2.6}$$

$$\epsilon_p = \frac{\rho_{0p}{b_p}^2}{\rho_{0A}{b_A}^2} \tag{2.7}$$

They also satisfy an initial condition:

$$Q_p(\mathbf{r},0|\mathbf{r}') = \sum_n \delta(\mathbf{r} - \mathbf{r}' - \mathbf{R}_n) \tag{2.8}$$

The potentials $\omega_p(\mathbf{r})$ can be written

$$\omega_A(\mathbf{r}) = \chi r_C[\phi_B(\mathbf{r}) - \bar{\phi}_B] + \eta(\mathbf{r}) \tag{2.9}$$

$$\omega_B(\mathbf{r}) = \chi r_C[\phi_A(\mathbf{r}) - \bar{\phi}_A] + \eta(\mathbf{r}) \tag{2.10}$$

where $\eta(\mathbf{r})$ is related to a Lagrange multiplier field associated with the incompressibility condition. Since $\epsilon_A = 1$, we simplify the notation by denoting $\epsilon_B \equiv \epsilon$, as given in eq 1.3.

It was sufficient to solve for Q_p in one unit cell. The local volume fractions are given by convolutions such as the following for $\phi_A(\mathbf{r})$

$$\phi_A(r) = f_A\frac{V}{Q_C}\int_0^1 d\tau\, q_A(r,\tau)\tilde{q}_A(r,1-\tau) \tag{2.11}$$

where

$$q_p(r,\tau) = \int_\Omega d\mathbf{r}'\, Q_p(\mathbf{r},\tau|\mathbf{r}') \tag{2.12}$$

$$\tilde{q}_A(r,1-\tau) = \int d\mathbf{r}'\, Q_A(\mathbf{r},1-\tau|\mathbf{r}')q_B(\mathbf{r}',1) \tag{2.13}$$

which depend only on a single variable, r, rather than the three component vector $\mathbf{r}$. Finally,

$$\frac{QC}{V} = \frac{m}{\alpha_m(1)}\int_0^1 \alpha_m(r)\, dr\, q_A(r,1)q_B(r,1) \tag{2.14}$$

where $m = 1$, 2, or 3 for layers, cylinders, or spheres, respectively, and $\alpha_1(r) = 1$, $\alpha_2(r) = 2\pi r$, and $\alpha_3(r) = 4\pi r^2$.

Equations 2.5–2.14 constitute a self-consistent problem for a given structure and lattice parameter. When it was solved, the free energy density was calculated via[26]

$$\frac{\Delta F}{\rho_0k_BTV} = \frac{1}{r_C}\left[\frac{m}{\alpha_m(1)}\int_0^1 \alpha_m(r)\, dr\, \{\chi r_C[\phi_A(r)\phi_B(r) - \bar{\phi}_A\bar{\phi}_B] - \omega_A(r)\phi_A(r) - \omega_B(r)\phi_B(r)\} - \ln\left(\frac{Q_C}{V}\right)\right] \tag{2.15}$$

For each structure, the procedure was repeated in order to minimize ΔF with respect to R, and then the equilibrium structure was identified. In strong segregation, we found the phase boundaries by fixing χr_c and calculating the free energies as functions of f_A. For a given χr_c, we estimate the numerical precision in the phase boundaries to be $\Delta f_A \simeq \pm 0.002$. In weak segregation, it was better to hold f_A constant and vary χr_c. In this regime, the numerical uncertainty in the phase boundaries is about $\Delta\chi r_c \simeq \pm 0.05$ for the diagram with $\epsilon = 0.6$, and $\Delta\chi r_c \simeq \pm 0.1$ for the one with $\epsilon = 0.1$.

3. Results and Discussion

Figure 1 shows the phase diagram we have calculated for a system with $\epsilon = 0.6$, which is equivalent to $\epsilon = (0.6)^{-1} = 1.67$ via the interchange of A and B. It can be compared directly with Figure 1 of ref 6, which was calculated in exactly the same way but for systems with $\epsilon = 1$. This comparison illustrates explicitly the effects of the conformational asymmetry.

The first notable result is that the order–disorder boundary was modified only slightly. At $\chi r_c = 80$, it is essentially symmetric, occurring at $f_A = 0.06$ and 0.94, which are the same values we found for $\epsilon = 1$. For smaller values of χr_c, this boundary remains nearly symmetric, curving and reaching a minimum which we calculate to be at $\chi r_c = 10.51 \pm 0.05$ and $f_A = 0.502 \pm 0.003$. These are essentially the same as for the conformationally symmetric case.

By contrast, the order–order boundaries are asymmetric and are shifted toward higher A content for this case of $\rho_{0B}{b_B}^2 < \rho_{0A}{b_A}^2$. At $\chi r_c = 80$, the $S_A \leftrightarrow C_A$ boundary has moved from 0.13 to 0.20, the $C_A \leftrightarrow L$ from 0.33 to 0.40, the $L \leftrightarrow C_B$ from 0.67 to 0.74, and the $C_B \leftrightarrow S_B$ from 0.87 to 0.92. (S_A denotes a set of spheres with cores consisting primarily of A blocks, etc.) In this region, the asymmetry has resulted in an L region centered at $f_A = 0.57$ rather than at 0.50, and an S_A region which is about 3 times wider than the S_B region.

This sequence of phase boundaries can be compared directly with those calculated by Helfand and Wasserman[6] for the strong segregation limit, which correspond to $\epsilon \simeq 0.7$ with the identification of the A and B blocks as PBD and PS, respectively. Beginning with $S_A \leftrightarrow C_A$ and moving across horizontally, they found the order–order transitions at weight fractions of about 0.15, 0.35, 0.7, and 0.9. These compare with our sequence of about 0.20, 0.40, 0.74, and 0.92; the slightly smaller asymmetry they found is consistent with their slightly larger value of ϵ.

The shift in the phase boundaries toward higher A content can be understood physically by considering the competing effects of the two controlling factors. On the basis of volume fractions alone, one would expect the center of stability of the L phase to be at $f_A = 0.5$. For such a copolymer, the two sublayers would be of equal thicknesses, $d_A = d_B$. However, if the copolymers were conformationally asymmetric, then the deformation of the two blocks, relative to their unperturbed dimensions, would be unequal. For the case $\epsilon < 1$ considered explicitly here, the B blocks would be more stretched than the A blocks. This difference would be reduced if d_A were increased relative to d_B, which would require $f_A > f_B$. Hence this effect tends to shift the center of stability toward higher f_A. An upper limit on the size of this size can be estimated by supposing that, of themselves, the coil statistics would tend to place the center of stability at the point where the two sublayer thicknesses are in proportion to their corresponding unperturbed radii of gyration. Equating d_A/d_B with f_A/f_B, and using eq 1.2 for the radii of gyration, this is equivalent to

$$\frac{f_A}{f_B} = \frac{{Z_A}^{1/2}b_A}{{Z_B}^{1/2}b_B} \tag{3.16}$$

which can be trivially rearranged and solved to yield $f_A = 1/(1 + \epsilon)$ for this upper limit. The two effects together

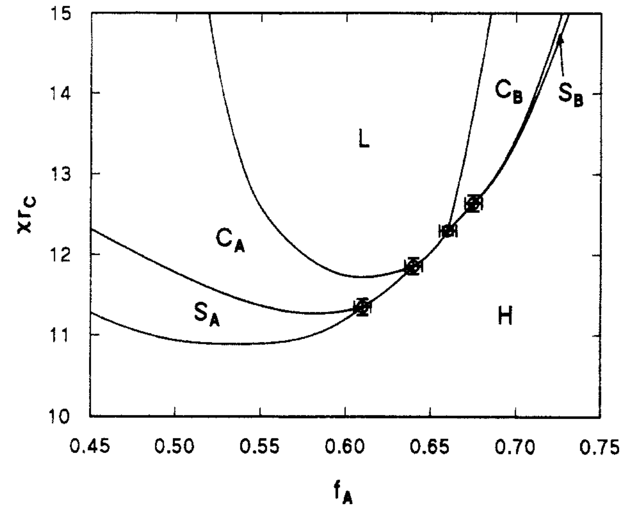

Figure 2. Part of the calculated phase diagrams for copolymers with highly asymmetric coil statistics chosen so that $\epsilon = 0.1$.

suggest that the L phase should be centered around a value of f_A satisfying

$$\frac{1}{2} \le f_A \le \frac{1}{1+\epsilon} \qquad (3.17)$$

(for this choice $\epsilon \le 1$). For the case shown in Figure 1, this implies $0.5 \le f_A \le 0.63$; the actual center, $f_A \simeq 0.57$, falls just about in the middle of this interval.

Returning to the phase diagram, as χr_c is reduced, the initial changes in the order–order phase boundaries are qualitatively the same as those for $\epsilon = 1$. Quantitatively, there is an interesting difference between the $C_A \leftrightarrow L$ and $L \leftrightarrow C_B$ boundaries. The former is noticeably less dependent on f_A, down to about $\chi r_c \simeq 20$.

Continuing down into the weak segregation regime, the phase boundaries curve in a way which is initially qualitatively consistent with the case of $\epsilon = 1$. However, they differ in two ways. First, the minimum of each curve is shifted slightly to $f_A > 0.5$. Second, small windows are opening up on one side of the phase diagram, the largest being an $H \leftrightarrow C_A$ window centered at about $f_A \simeq 0.547$. However, the width of each window is on the same order as the numerical uncertainty in the positions of the phase boundaries, and we were unable to resolve them with any degree of precision.

In order to amplify these windows and exhibit their origin, we carried out a series of calculations for a model system with highly asymmetric coil statistics, choosing $\epsilon = 0.1$. The microphase diagram in the vicinity of the MST is shown in Figure 2, which clearly shows the existence of $H \leftrightarrow C$ and $H \leftrightarrow L$ windows. The MST reaches a minimum value of about $\chi r_c \simeq 10.9$, occurring at about $f_A \simeq 0.54$, as compared with $\chi r_c = 10.5$ at $f_A = 0.5$ for the $\epsilon = 1$ case. However, the nature of the transition at this minimum differs, being a first order $H \leftrightarrow S_A$ transition. In fact, there are windows from the H to each of the ordered microphases: $H \leftrightarrow S_A$ for $f_A \lesssim 0.61$, $H \leftrightarrow C_A$ for $0.61 \lesssim f_A \lesssim 0.64$, $H \leftrightarrow L$ for $0.64 \lesssim f_A \lesssim 0.66$, $H \leftrightarrow C_B$ for $0.66 \lesssim f_A \lesssim 0.675$, and $H \leftrightarrow S_B$ for $f_A \gtrsim 0.675$.

It is interesting to note that this phase diagram for A–B diblock copolymers of high conformational asymmetry bears some resemblance to ones which were calculated for A–B–A triblock copolymers by Mayes and Olvera de la Cruz.[14] They treated conformationally symmetric copolymers, i.e., $\rho_{0A} = \rho_{0B}$ and $b_A = b_B$, but allowed for all three blocks to be of unequal degrees of polymerization. In particular, the choice $Z_{A1} \neq Z_{A2}$ introduces an asymmetry into the molecules, of a somewhat different nature than conformational asymmetry. The current Figure 2 most resembles Figure 2 of that paper, which is for $Z_{A1} = Z_{A2}/3$. In both diagrams, the overall minimum in the order–disorder boundary is displaced away from $f_A = 0.5$, although to $f_A > 0.5$ in the present case and to $f_A < 0.5$ in theirs. In both cases, the $H \leftrightarrow L$ transition is displaced to $f_A > 0.5$, which is to the right of the minimum in the MST on each diagram. An important qualitative difference is the finite width of the $H \leftrightarrow L$ and $H \leftrightarrow C$ windows in the present diagram, features not present in theirs. As well, the $L \leftrightarrow C$ boundaries are generally steeper, and the S_A region in particular is considerably larger.

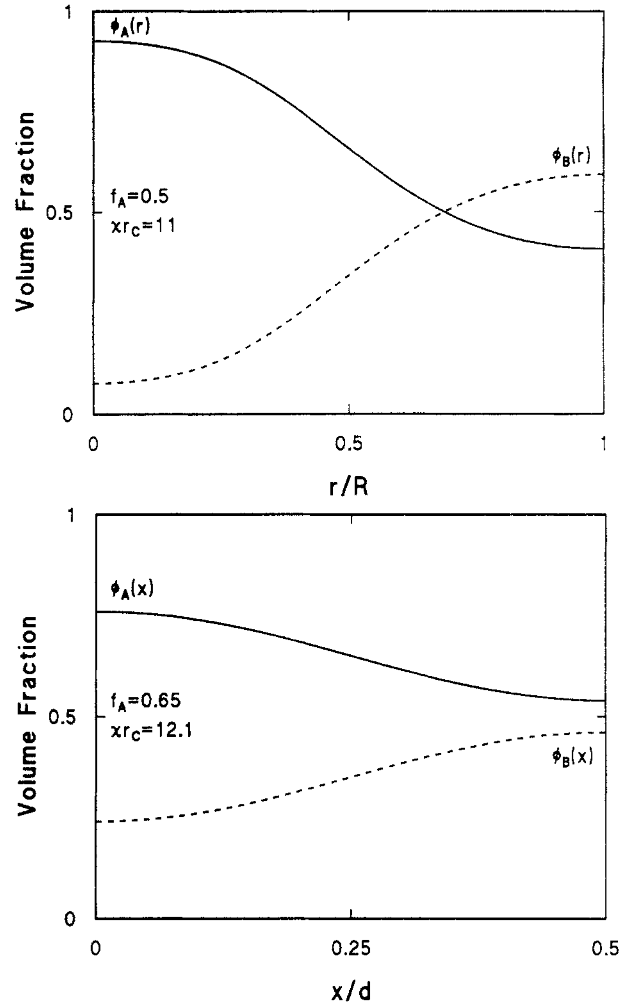

Figure 3. (a) Calculated density profiles $\phi_A(r)$ and $\phi_B(r)$ for copolymers with equal volume fractions for each block, but with high conformational asymmetry characterized by $\epsilon = 0.1$. This system corresponds to a point on the phase diagram lying essentially at the MST. The structure in this case is spheres centered at $r = 0$, with the A block forming the cores. For this geometry, the proportion of each component a distance r from the origin is proportional to $4\pi r^2\phi(r)$. (b) Calculated density profiles $\phi_A(x)$ and $\phi_B(x)$ for copolymers with unequal volume fractions, as shown, and with high conformational asymmetry characterized by $\epsilon = 0.1$. This system corresponds to a point on the phase diagram lying essentially at the MST. The structure in this case is layers, and half the unit cell is shown.

The nature of the order–disorder transition for conformationally asymmetric copolymers is illustrated in Figure 3, which shows the calculated density profiles corresponding to two points on the MST on Figure 2. The first is at $f_A = 0.5$, and the second is at $f_A = 0.65$, which is the center of the calculated $H \leftrightarrow L$ window. We chose these points to facilitate comparison with conformationally symmetric systems. For those systems, $f_A = 0.5$ corresponds to a second order $H \leftrightarrow L$ transition (in mean field theory), and the density variations reduce to simple cosine functions with amplitudes which vanish at the transition. By contrast, Figure 3a shows that the transition at $f_A = 0.5$, which is $S_A \leftrightarrow H$, is first order, and in fact the amplitude of the variation in each profile is large. For example, $\phi_A(r)$ varies from a value of about 0.92 at the center of the core, to about 0.40 at the edge of the unit cell. The other profile, $\phi_B(r)$, complements this as $\phi_B(r) = 1 - \phi_A(r)$. In Figure 3b we see that the H ↔ L transition is also first order. In this case, each density profile consists, approximately, of a cosine-like variation about its average value, with equal amplitudes of about 0.11. This corresponds to about 31% of the overall value of $\bar{\phi}_B$, and about 17% of $\bar{\phi}_A$.

In summary, we have shown that, within mean field theory, the effects of conformational asymmetry on the microphase diagram of an A-*b*-B diblock copolymer can be characterized by a single parameter, which we labeled $\epsilon = \rho_{0B}b_B^2/\rho_{0A}b_A^2$. There should be no "universal" two dimensional phase diagram, but for a given value of ϵ, the phase diagram can be expressed in terms of χr_c and f_A, where r_c is an effective degree of polymerization. As a consequence, we suggest that any experimentally determined phase diagram should be characterized by the corresponding conformational asymmetry, i.e., ϵ. The value of ϵ can be restricted to lie either below or above unity, through the arbitrary labeling of the blocks. With the choice $\epsilon \leq 1$, we found that typical values for the Kuhn lengths and reference densities indicate a realistic range for ϵ of $0.3 \lesssim \epsilon \leq 1$. We calculated the phase diagram for $\epsilon = 0.6$, finding the order–disorder boundary to be virtually unaffected by the conformational asymmetry, but all the order–order boundaries to be shifted toward higher *A* content. In the strong segregation regime, the S_A region is about 3 times broader than the S_B region, and the C_A region about 50% broader than the C_B region. The phase boundaries are in reasonable agreement with the experimental values for PS-*b*-PI in strong segregation, although it is not clear how asymmetric these copolymers actually are. Finally, we found that conformational asymmetry leads to direct H ↔ C and H ↔ L windows on one side of the phase diagram ($f_A > 0.5$), even without fluctuation effects.

Acknowledgment. We thank Ms. Jun Ren for help with the numerical calculations. The work was supported in part by the National Sciences and Engineering Research Council of Canada.

References and Notes

(1) Hasegawa, H.; Tanaka, H.; Yamasaki, K.; Hashimoto, T. *Macromolecules* **1987**, *20*, 1651.
(2) Thomas, E. L.; Alward, D. B.; Kinning, D. L.; Martin, D. L.; Handlin, D. L., Jr.; Fetters, L. J. *Macromolecules* **1986**, *19*, 2197.
(3) Almdal, K.; Koppi, K. A.; Bates, F. S.; Mortensen, K. *Macromolecules* **1992**, *25*, 1743.
(4) Almdal, K.; Bates, F. S.; Förster, S.; Gehlsen, M. D.; Hamley, I. W.; Khandpur, A.; Koppi, K. A.; Mortensen, K.; Rosedale, J. H.; Schulz, M. F. APS March Meeting, Seattle, 1993.
(5) Whitmore, M. D.; Vavasour, J. D. *Macromolecules* **1992**, *25*, 2041.
(6) Vavasour, J. D.; Whitmore, M. D. *Macromolecules* **1992**, *25*, 5477.
(7) Bates, F. S. *Science* **1991**, *251*, 845.
(8) Förster, S.; Khandpur, A.; Schulz, M. F.; Bates, F. S. APS March Meeting, Seattle, 1993.
(9) Helfand, E.; Wasserman, Z. R. In *Developments in Block Copolymers*; Goodman, I., Ed.; Elsevier: New York, 1982; Vol. 1.
(10) Leibler, L. *Macromolecules* **1980**, *13*, 1602.
(11) Fredrickson, G. H.; Helfand, E. *J. Chem. Phys.* **1987**, *87*, 697.
(12) Mayes, A. M.; Olvera de la Cruz, M. *Macromolecules* **1991**, *24*, 3975.
(13) Olvera de la Cruz, M. *Phys. Rev. Lett.* **1991**, *67*, 85.
(14) Mayes, A. M.; Olvera de la Cruz, M. *J. Chem. Phys.* **1991**, *95*, 4670.
(15) Tang, H.; Freed, K. F. *Macromolecules* **1991**, *24*, 958.
(16) Dudowicz, J.; Freed, K. F. *Macromolecules* **1993**, *26*, 213.
(17) Tanaka, H.; Sakurai, S.; Hashimoto, T.; Whitmore, M. D. *Polymer* **1992**, *33*, 1006.
(18) Matsushita, Y.; Mori, K.; Saguchi, R.; Nakao, Y.; Noda, I.; Nagasawa, M. *Macromolecules* **1990**, *23*, 4313.
(19) Tanaka, H.; Hashimoto, T. *Macromolecules* **1991**, *24*, 5398.
(20) Owens, J. N.; Gancarz, I. S.; Koberstein, J. T.; Russel, T. P. *Macromolecules* **1989**, *22*, 3380.
(21) Richardson, M. J.; Savill, N. J. *Polymer* **1977**, *18*, 3.
(22) Sakurai, S.; Mori, K.; Okawara, A.; Kimishima, K.; Hashimoto, T. *Macromolecules* **1992**, *25*, 2679.
(23) Brandrup, J., Immergut, E. H., Eds. *Polymer Handbook*, 2nd ed.; Interscience: New York, 1975.
(24) Anastasiadis, S. H.; Russell, T. P.; Satija, S. K.; Majkrzak, C. F. *J. Chem. Phys.* **1990**, *92*, 5677.
(25) Rigby, D.; Roe, R.-J. *Macromolecules* **1986**, *19*, 721.
(26) Note that in the expression for the free energy given in ref 6 (eq 36) the term involving $\bar{\phi}_A\bar{\phi}_B$ was inadvertently dropped.